Open access • Journal Article • DOI:10.1016/J.COLSURFB.2016.11.027

Chitosan nanoparticles as carrier systems for the plant growth hormone gibberellic acid — Source link ⧉

Anderson do Espirito Santo Pereira, Paula Mayara Silva, Jhones Luis de Oliveira, Halley Caixeta Oliveira ...+2 more authors

Institutions: State University of Campinas, Sao Paulo State University

Related papers:

- Chitosan nanoparticle based delivery systems for sustainable agriculture.

- γ-Polyglutamic acid/chitosan nanoparticles for the plant growth regulator gibberellic acid: Characterization and evaluation of biological activity

- Cu-chitosan nanoparticle boost defense responses and plant growth in maize (Zea mays L.)

- Chitosan/tripolyphosphate nanoparticles loaded with paraquat herbicide: An environmentally safer alternative for weed control

- Polymeric nanoparticles as an alternative for application of gibberellic acid in sustainable agriculture: a field study.

Full Length Article

Chitosan nanoparticles as carrier systems for the plant growth hormone gibberellic acid

Anderson Espirito Santo Pereira [a,b], Paula Mayara Silva [b], Jhones Luis Oliveira [b], Halley Caixeta Oliveira [c], Leonardo Fernandes Fraceto [a,b,*]

[a] Department of Biochemistry, State University of Campinas (UNICAMP), Campus Universitário Zeferino Vaz, s/n, Cidade Universitária, CEP 13083-870, Campinas, SP, Brazil
[b] Department of Environmental Engineering, Institute of Science and Technology of Sorocaba (ICTS), São Paulo State University (UNESP), Avenida Três de Março, 511, CEP 18087-180, Sorocaba, SP, Brazil
[c] Department of Animal and Plant Biology, University of Londrina, PR 445, km 380, CEP 86057-970, Londrina, PR, Brazil

ABSTRACT

This work concerns the development of nanocarriers composed of alginate/chitosan (ALG/CS) and chitosan/tripolyphosphate (CS/TPP) for the plant growth regulator gibberellic acid (GA$_3$). ALG/CS nanoparticles with and without GA$_3$ presented mean size of 450 ± 10 nm, polydispersity index (PDI) of 0.3, zeta potential of -29 ± 0.5 mV, concentrations of 1.52×10^{11} and 1.92×10^{11} nanoparticles mL^{-1}, respectively, and 100% encapsulation efficiency. CS/TPP nanoparticles with and without GA$_3$ presented mean size of 195 ± 1 nm, PDI of 0.3, zeta potential of $+27 \pm 3$ mV, concentrations of 1.92×10^{12} and 3.54×10^{12} nanoparticles mL^{-1}, respectively, and 90% encapsulation efficiency. The nanoparticles were stable during 60 days and the two systems differed in terms of the release mechanism, with the release depending on factors such as pH and temperature. Bioactivity assays using *Phaseolus vulgaris* showed that the ALG/CS-GA$_3$ nanoparticles were most effective in increasing leaf area and the levels of chlorophylls and carotenoids. The systems developed showed good potential, providing greater stability and efficiency of this plant hormone in agricultural applications.

© 2016 Elsevier B.V. All rights reserved.

1. Introduction

Plant growth regulators (PGRs) are a class of natural or synthetic compounds based on plant hormones. They have broad applications in agriculture and horticulture, where they are used to modulate plant growth and development, hence increasing yields and the quality of crop products [1]. These compounds are used at low concentrations, acting at the cellular level during different stages of plant development, and include gibberellins, auxin, cytokinins, jasmonic acid, and ethylene, amongst others [2].

Gibberellins are a class of tetracyclic diterpenoid plant hormones involved in several physiological processes in plants [3]. GA$_3$ became one of the most popular PGRs used in agriculture to break seed dormancy, promote shoot elongation, induce organ differentiation, and increase the number and weight of fruit [4–6].

A difficulty is that PGRs can readily degrade when exposed to environmental factors such as light and temperature, resulting in loss of activity. In this context, one of the uses of nanotechnology in agriculture is to provide nanoscale materials able to enhance the stability and activity of various active agents, while at the same time reducing environmental impacts [7–11]. For example, the encapsulation of agrochemicals in nanoparticles can improve their physicochemical properties and reduce problems such as sorption and leaching, thus increasing bioavailability and efficiency, while reducing the concentrations required and making the products safer in the environment [12–14].

Nanocarrier systems based on chitosan (CS) have a range of applications for crop protection. Nanoparticles produced using various techniques can be employed as delivery systems for pesticides and fertilizers, as well as for gene delivery [15]. The nanoparticle itself may present fungicidal activity, depending on the molecular weight of CS, nanoparticle size, and the zeta potential [16]. The use of CS nanoparticles loaded with paraquat resulted in reduced toxicity of the herbicide, enabling weed control with less harm to the environment [12]. CS nanoparticles prepared with the addition of anionic proteins isolated from *Penicillium oxalicum* can be used in

the treatment of seeds for fungus control, while at the same time improving plant development [17].

Another application of nanoparticles composed of CS is to enhance the solubility, stability, and cellular uptake of antioxidant compounds, increasing their applications in the food and pharmaceutical industries [18]. Nanocarrier systems have been developed for plant growth regulators such as brassinosteroids [19] and O-naphthylacetyl [20]. Liu et al. [21] showed that the association of gibberellic acid and CS generated a sustained release system, increasing the solubility of the active agent and protecting against thermal and photolytic degradation at different pH values.

Nanoparticles of alginate/chitosan (ALG/CS) and chitosan/tripolyphosphate (CS/TPP) have been used as carriers of drugs and agrochemicals in sustained release systems that can extend the duration of action of the active chemical and improve its stability [12,22–24]. The CS polymer is a cationic polysaccharide derived from the deacetylation of chitin [25]. It has many applications in agriculture, with properties including fungicidal activity and the enhancement of plant defense mechanisms [15]. The alginate polymer (ALG), extracted from brown algae, is non-toxic, biocompatible, biodegradable, and possesses a characteristic negative charge, due to the presence of uronic acid groups [26].

In this work, ALG/CS and CS/TPP nanoparticles were used to prepare two different carrier systems for the GA$_3$ plant hormone that could provide greater efficiency and stability in the field, leading to improved quality and yield of agricultural products. Physicochemical characterization of the systems considered the following parameters: size distribution (DLS and NTA measurements), polydispersity index (PDI), zeta potential, and encapsulation efficiency. The profiles of GA$_3$ release from the nanoparticles were determined under different conditions. Fourier transform infrared spectroscopy (FTIR) and differential scanning calorimetry (DSC) measurements were performed in order to investigate possible interactions between the hormone and the components of the nanoparticles, and the biological activities of the systems were evaluated in *Phaseolus vulgaris*.

2. Experimental

2.1. Materials

The GA$_3$ plant hormone, sodium alginate, chitosan (MW: 27 kDa; degree of deacetylation: 75–85%), and tripolyphosphate were purchased from Sigma-Aldrich. Acetonitrile and acetic acid (HPLC grade) were obtained from JT Baker. Ultrafiltration filters and cellulose membranes were purchased from Millipore. The seeds of *Phaseolus vulgaris* L. (Fabaceae) were collected in the field, in the municipality of São Miguel Arcanjo (São Paulo, Brazil).

2.2. Preparation of the ALG/CS and CS/TPP nanoparticles

2.2.1. ALG/CS nanoparticles

The ALG/CS nanoparticles were prepared by the ionotropic pregelation method [22]. Firstly, a peristaltic pump was used to slowly add 3.75 mL of CaCl$_2$ solution to 59 mL of ALG solution (0.063%, pH 4.9), under vigorous stirring. The GA$_3$ plant hormone was then added to give a final concentration of 50 µg mL^{-1}. This solution was kept under vigorous stirring and a peristaltic pump was used to add 12.5 mL of CS solution (0.07%, pH 4.6), prepared in an aqueous solution containing 5.7% acetic acid, over a period of 90 min. The same procedure was performed without the presence of the hormone.

2.2.2. CS/TPP nanoparticles

The CS/TPP nanoparticles were prepared by the gelation method [27], with modifications. Firstly, 10 mL of a solution of CS (0.2%, pH 4.5), prepared in an aqueous solution of 0.6% acetic acid, was kept under vigorous stirring and the GA$_3$ hormone was added to give a final concentration of 50 µg mL^{-1}. After dissolution of the hormone, 6 mL of TPP solution (0.1%, pH 4.5 at 4 °C) was added. Nanoparticles were also prepared without the presence of the hormone.

2.3. Characterization of the nanoparticles

The ALG/CS and CS/TPP formulations were analyzed periodically during 60 days, considering the following variables: size, polydispersity index, zeta potential, and pH.

2.3.1. Nanoparticle tracking analysis (NTA)

The NTA technique was used to determine the size distribution and concentration of the nanoparticles in the formulations, using a Model LM-10 instrument (Malvern Instruments, UK). For the analysis, 10 µL volumes of the nanoparticle formulations (ALG/CS or CS/TPP) were diluted in 990 µL of deionized water. Each sample was measured 10 times, with approximately 400 particles counted in each measurement. The analyses were performed at 25 °C.

2.3.2. Dynamic light scattering

The size distribution and polydispersity index (PDI) of the nanoparticles were determined by the dynamic light scattering (DLS) technique, using a Zetasizer Nano ZS90 instrument (Malvern Instruments, UK). The samples were analyzed in triplicate, at 25 °C, with the scattered light detected at an angle of 90°.

2.3.3. Atomic force microscopy (AFM)

Nanoparticle images were obtained with an Easy Scan 2 Basic AFM instrument (Nanosurf, Switzerland), operated in contact mode using TapAl-G cantilevers (BudgetSensors, Bulgaria) to scan the samples. The nanoparticles were previously dialyzed for 1 h using a cellulose membrane with 1 kDa exclusion pore size, followed by dilution at 1:7000 in ultrapure water.

2.3.4. Zeta potential

The zeta potential values (in mV) were determined by electrophoresis, with analysis in triplicate, at 25 °C, using the Zetasizer ZS90 instrument.

2.3.5. Chemical stability of the polymers (pH)

Measurements of pH were used to assess possible degradation of the components of the formulations, using a Tecnal pH meter that had been previously calibrated. Samples were assessed in triplicate, at 25 °C.

2.3.6. Encapsulation efficiency

The encapsulation efficiency was determined indirectly. Soon after preparation of the nanoparticles containing GA$_3$, a 400 µL volume was transferred to an ultrafiltration device (Microcon, Millipore) containing a regenerated cellulose membrane with an exclusion pore size of 30 kDa. The samples were centrifuged for 30 min at 200g. The filtrate was collected and analyzed by high performance liquid chromatography (HPLC) in order to quantify the hormone that was not associated with the nanoparticles. The encapsulation percentage was then obtained from the concentration in the filtrate, considering 100% to be 50 µg mL^{-1}.

2.3.6.1. Methodology for quantification of GA$_3$. Quantification of GA$_3$ was performed using a Varian ProStar HPLC equipped with a Model 210 pump, a Model 325 UV–vis detector, a Metatherm oven, and an autosampler. The column was a Supelcosil LC$_{18}$-DB (3.3 × 4.6 cm; 3 µm) and the mobile phase was acetonitrile and water (containing 0.1% phosphoric acid (H$_3$PO$_4$)) at a ratio of 3:1 (v:v), pumped at a flow rate of 0.4 mL min^{-1}. The detector wavelength (λ) was 210 nm. The chromatograms were processed using

Galaxy Workstation software. The calibration curve obtained under these conditions could be described by $y = 9.46 + 2.6^*x$ ($r = 0.998$), and the limits of detection and quantification were 4.16 and 13.89 μg mL^{-1}, respectively.

2.3.7. Differential scanning calorimetry (DSC)

The samples were placed in aluminum cups and analyzed by DSC under a flow of nitrogen at 50 mL min^{-1}, with heating from 20 to 350 °C at a rate of 10 °C min^{-1}.

2.4. Release kinetics assays and mathematical modeling

2.4.1. Release kinetics

The release kinetics experiments employed a system with acceptor and donor compartments separated by a cellulose membrane with 1 kDa exclusion pore size. Samples of free GA$_3$ (diluted in distilled water) or nanoparticles with GA$_3$ were placed in the donor compartment. In the case of the ALG/CS-GA$_3$ nanoparticles, the acceptor compartment contained CaCl$_2$ solution (11 mM, pH 4.9), while TPP solution (0.1%, pH 4.75) was used for the CS/TPP-GA$_3$ nanoparticles. Distilled water was used for the system with free GA$_3$. Magnetic stirring was maintained throughout the experiments. After addition of the samples to the donor compartment, aliquots were periodically collected from the acceptor compartment. The assays were performed in triplicate, at room temperature.

2.4.2. Release assays at different pH and temperature

The release of GA$_3$ under different conditions was investigated by altering the pH and temperature. The assays were performed as described in Section 2.4.1, at 30 °C and at ambient temperature, altering the pH values to 5.9 and 5.7 for the ALG/CS-GA$_3$ and CS/TPP-GA$_3$ nanoparticles, respectively. The pH of the acceptor system was the same as that of the nanoparticle suspension. After the release assay, characterization was performed of the nanoparticles present in the donor compartment.

2.4.3. Korsmeyer-Peppas mathematical model

The mechanism of release of GA$_3$ from the nanoparticles was elucidated using the Korsmeyer-Peppas model, described by:

$$M_t/M_\infty = kt\mathrm{n} \tag{1}$$

where M_t is the amount of GA$_3$ released as a function of time (t), M_∞ is the amount of GA$_3$ added to the system at $t = 0$, k is the kinetic constant, and n is the release exponent. For the application of the mathematical model, only release values lower than 60% were used [28]. The mathematical model was applied to the results obtained under the different conditions in order to elucidate the effects of pH and temperature on the profiles of release from the nanoparticles.

2.5. Biological activity

In agriculture, GA$_3$ is used in bean crops [29,30], so for this reason, *Phaseolus vulgaris* L. cv. Carioca (Fabaceae) was selected to evaluate the biological activities of the CS/TPP-GA$_3$ and ALG/CS-GA$_3$ nanoparticles, in comparison with the activities of the free active agent, the control (distilled water), and nanoparticles without GA$_3$. The seeds were treated for 1 h using 1 g of seeds and solutions of GA$_3$ at concentrations that provided GA$_3$:seed mass ratios of 0.05, 0.037, 0.025, and 0.012%. For the ALG/CS-GA$_3$ nanoparticles, the dilutions employed CaCl$_2$ solution (11 mM, pH 4.9), while TPP (0.1%, pH 4.75) was used for the CS-TPP-GA$_3$ nanoparticles. Distilled water was used in the case of the free GA$_3$. After the treatments, the seeds were sown in pots 9.3 cm high and with upper and lower diameters of 12.5 and 9.3 cm, respectively, filled with 600 g of California

substrate. The pots were kept in a greenhouse under natural conditions of light and temperature. Each treatment was performed in quadruplicate ($n = 4$). The plants were collected after 7 days and the root and shoot length and leaf area were evaluated, as well as the contents of chlorophyll 'a', chlorophyll 'b', and carotenoids.

2.5.1. Determination of chlorophyll 'a', chlorophyll 'b', and carotenoids

For each treatment, a sample of leaf with area of 5 mm^2 was obtained using a paper punch and stored for 12 h in an Eppendorf tube containing 2 mL of DMSO, protected from exposure to light. The measurements were made using a Varian Cary 50 UV–vis spectrophotometer operated at wavelengths of 665, 649, and 480 nm. The contents of chlorophyll 'a', chlorophyll 'b', and carotenoids were calculated using Eqs. (2)–(4), respectively.

$$\textbf{\textit{Chla}} = 12.19 x A665 - 3.45 x A649 \tag{2}$$

$$\textbf{\textit{Chlb}} = 21.99 x A649 - 5.32 x A665 \tag{3}$$

$$\textbf{\textit{Carotenoids}} = \frac{100 x A480 - 2.14 x Chla - 70.16 x Chl - b}{220} \tag{4}$$

where *Chl a* is the content of chlorophyll 'a', *Chl b* is the content of chlorophyll 'b', and *A* (followed by the wavelength) is the absorbance value obtained at each wavelength [31].

2.5.2. Data analysis

The results were calculated as means and standard deviations, with pretreatment according to Eq. (5):

$$\Delta = M^t - M^C \tag{5}$$

where M^t is the mean value obtained for the different treatments (ALG/CS, CS/TPP, GA$_3$, CS/TPP-GA$_3$, and ALG/CS-GA$_3$) and concentrations (0.05, 0.037, 0.025, and 0.012%), and M^C is the mean for the control. Statistical analysis of the effects of the different treatments employed one-way analysis of variance (ANOVA) with the Tukey post-hoc test, using a significance level of $p < 0.05$. These analyses were performed with Graphpad Prism v. 5.01 software.

3. Results and discussion

3.1. Characterization of the ALG/CS and CS/TPP nanoparticles

NTA analyses were used to determine the sizes and concentrations of the ALG/CS and CS/TPP nanoparticles, with and without GA$_3$. The concentrations were 1.52×10^{11} and 1.92×10^{11} particles mL^{-1} (Fig. 1a and b), and 1.92×10^{12} and 3.54×10^{12} particles mL^{-1} (Fig. 1c and d), respectively. Nanoparticle concentrations are rarely reported in the literature, but are important for determination of, for example, the toxicity of nanoparticles based on the number of particles, rather than on the concentration of the material used (polymer, lipid, metal, etc.) [32]. Nanoparticle size was determined by both NTA and DLS, with average values of 450 ± 10 nm for ALG/CS and 195 ± 1 nm for CS/TPP, with and without GA$_3$ (Fig. 1). Both techniques gave the same results for the average sizes of the ALG/CS and CS/TPP nanoparticles with and without GA$_3$, suggesting that the addition of the hormone did not affect the nanoparticle structure. The DLS peaks that appeared above 1000 nm for the ALG/CS nanoparticles with or without GA$_3$ could be attributed to aggregate formation.

Both techniques analyze the size of nanoparticles using their Brownian motion, although the NTA technique evaluates the size distribution by counting individual nanoparticles, while DLS measures the size distribution of the bulk nanoparticles [33]. The AFM images corroborated the sizes obtained using NTA and DLS and revealed that both types of nanoparticles were spherical (Figs. 2 and 3a). The use of NTA and DLS, together with AFM, helped
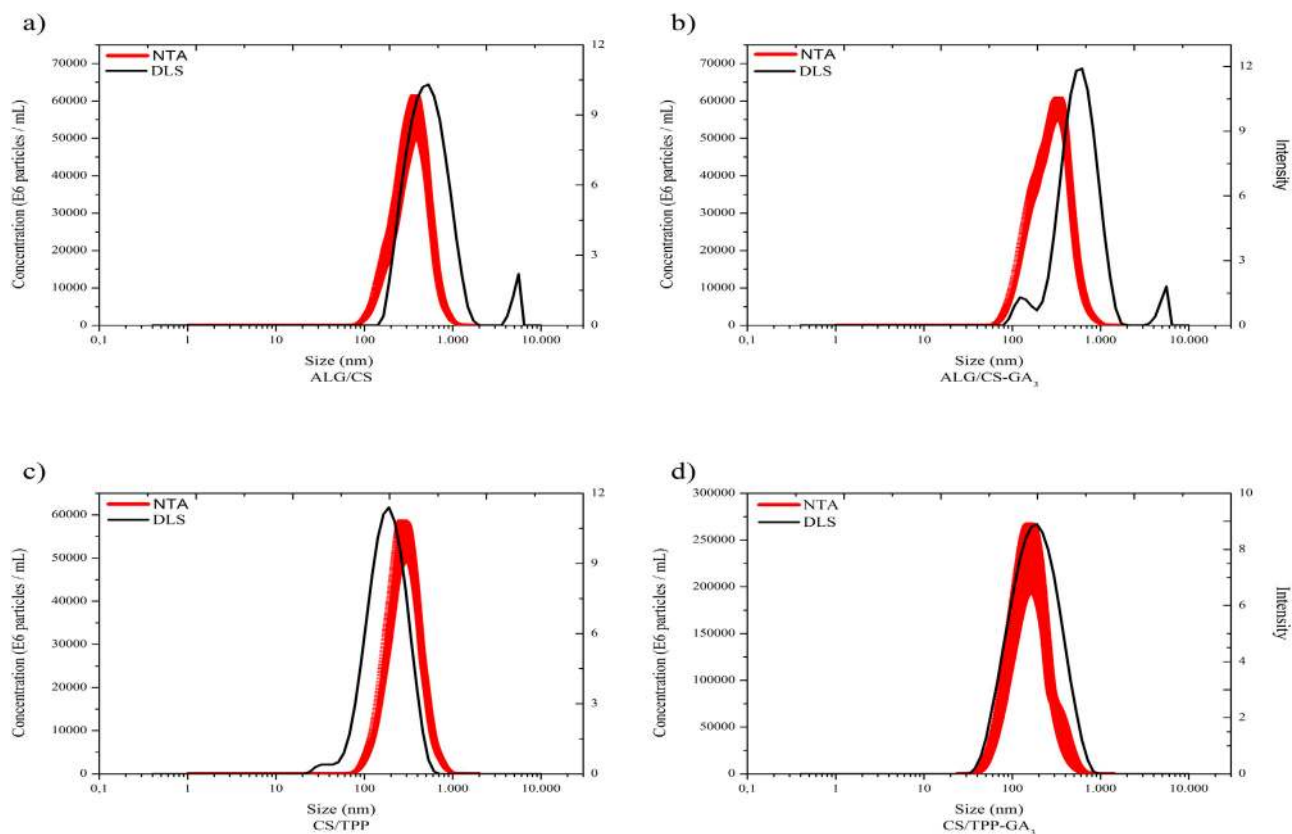
Fig. 1. Particle size analysis using the dynamic light scattering (DLS) and nanoparticle tracking analysis (NTA) techniques. a) ALG/CS, b) ALG/CS-GA$_3$, c) CS/TPP, and d) CS/TPP-GA$_3$. The samples were analyzed in triplicate, at 25 °C.
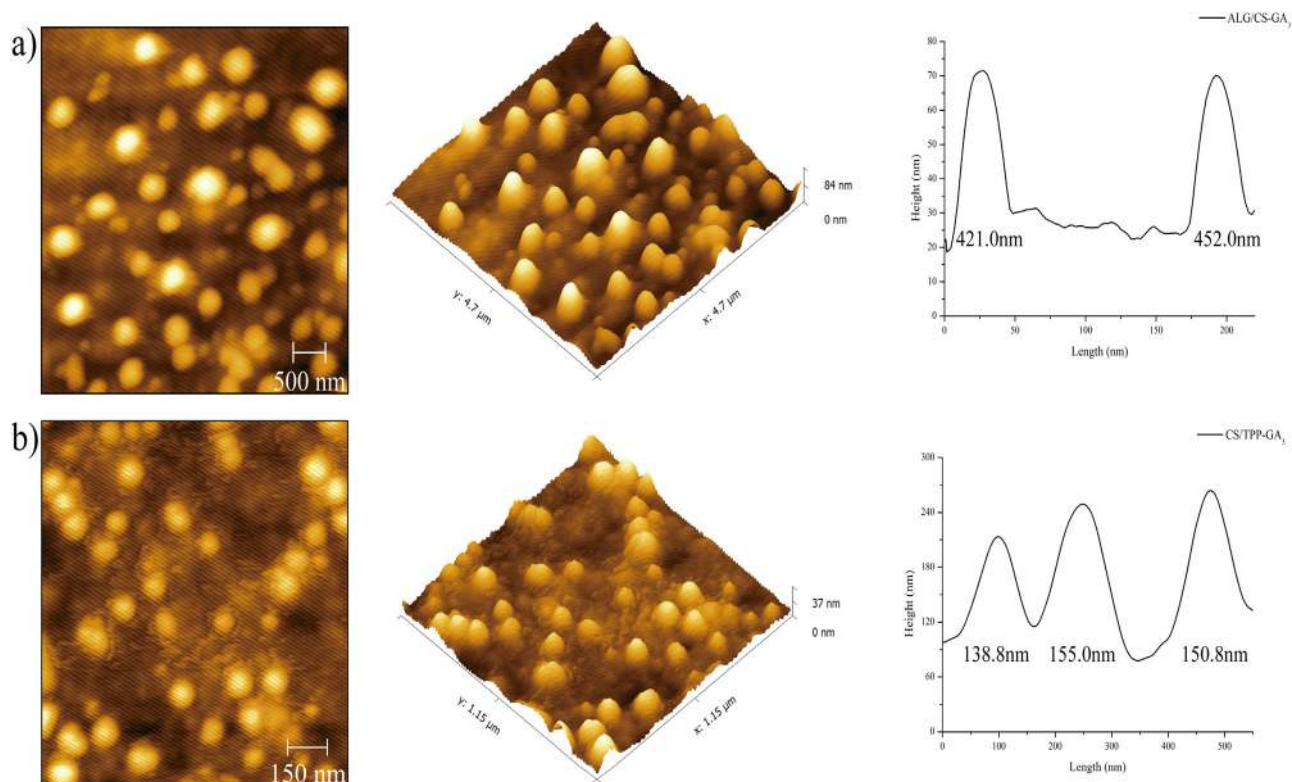

Fig. 2. Images obtained by atomic force microscopy (AFM) showing the spherical shape of the nanoparticles and the profile of size: a) ALG/CS and b) CS/TPP nanoparticles.
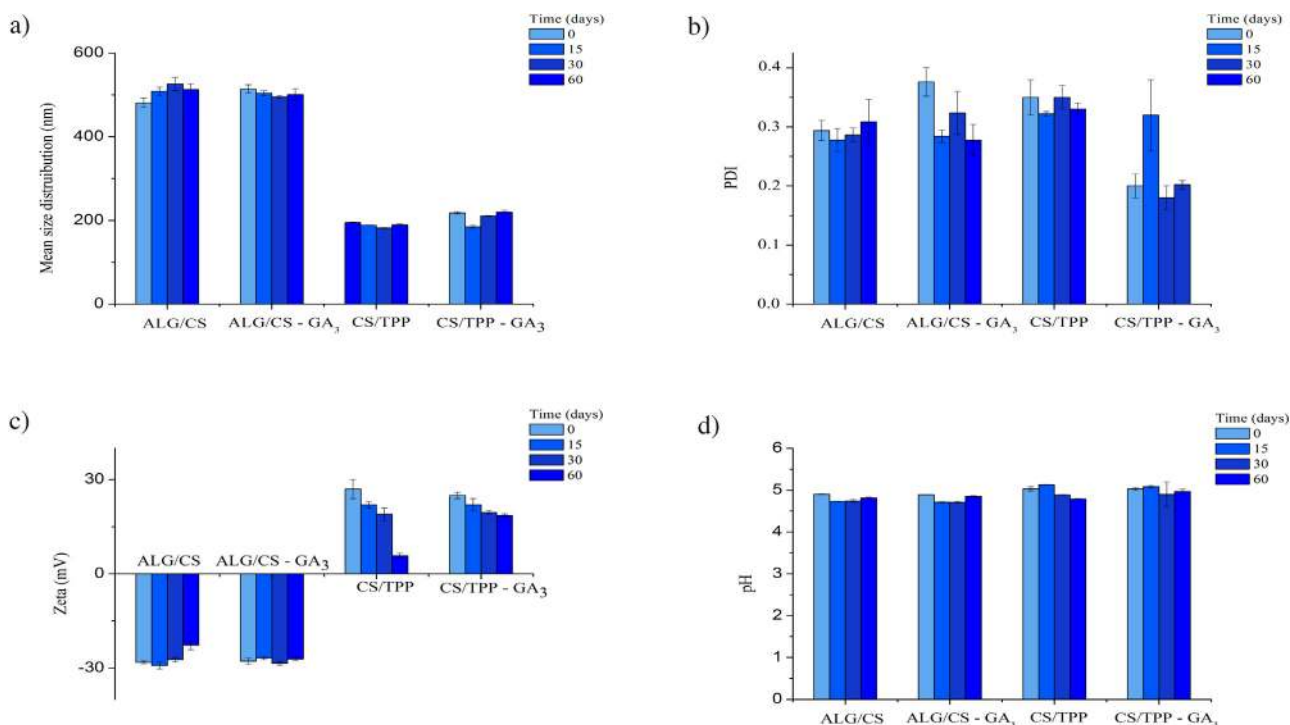
Fig. 3. Analysis of the stabilities of the ALG/CS and CS/TPP nanoparticles, with and without GA 3, over a period of 60 days, considering the variables: a) size, b) PDI, c) zeta potential, and d) pH. The samples were analyzed in triplicate, at 25 °C.

to validate the characterization of the sizes of the ALG/CS and CS/TPP nanoparticles.

The DLS technique was used to determine the PDI values (Fig. 3b). The mean value for the nanoparticles was 0.3, which is typical for these types of particles [12,34]. Nonetheless, the literature reports different sizes of ALG/CS nanoparticles, using the same technique. For example, Azevedo et al. [26] obtained nanoparticles with sizes of 100–120 nm, which were smaller than found here, and higher PDI of 0.4. Silva et al. [23] obtained particles in the 450–650 nm size range, with PDI values similar to those found in the present work. Different sizes have also been reported for CS/TPP nanoparticles. Vimal et al. [34] measured particles between 30 and 60 nm, while Rampino et al. [35] produced particles of similar size to those obtained in this study, but with lower PDI values of around 0.18-0.2.

The zeta potentials of the CS/TPP and ALG/CS nanoparticles were around 27 ± 3 mV and -29.0 ± 0.5 mV, respectively (Fig. 3c). The charges were related to the components used to produce the nanoparticles: the negative zeta potential of the ALG/CS nanoparticles was due to the carboxyl groups of ALG, which are ionized at pH 4.9 (COO^-) [36]; the positive charge of CS/TPP was due to the amino groups present in the CS polymer and exposed on the surfaces of the nanoparticles [35].

Another parameter evaluated was the final pH (Fig. 3d) of the formulations. In both cases, the pH was around 4.9, without any significant change over time, indicative of an absence of hydrolysis of the systems in the medium used here [37].

The efficiencies of encapsulation of GA$_3$ in the nanoparticles were 100% and 90% for ALG/CS and CS/TPP, respectively, demonstrating strong interaction of the hormone with these carriers. Intermolecular interactions involved the hydroxyl and carboxylic acid moieties present in the hormone molecule, which participated in hydrogen bonds and electrostatic linkages, respectively, with groups present in the polymers.

The use of CaCl$_2$ induces the formation of polymeric mesh, due to the interaction of Ca^{2+} ions with the carboxylic acid groups of

the ALG. The same groups are present in GA$_3$, so it can be inserted into the polymeric mesh by means of the same type of chemical interaction. Other studies have also reported the encapsulation of active chemicals due to their interactions with Ca^{2+} ions of ALG/CS nanoparticles [38,39].

For both CS/TPP and ALG/CS nanoparticles, the encapsulation can occur due to interactions involving free amino groups [40]. Another factor is the interaction between the active molecule and the surface of the nanoparticle [34]. For GA$_3$, both interactions may occur. Since the pka of this hormone is 4 and the pH of the formulation was 4.9, GA$_3$ was deprotonated and could interact with positive charges.

The temporal stabilities of the nanoparticles are shown in Fig. 3. The particle sizes and PDI values (Fig. 3a and b) showed no changes during the period evaluated. Increased size or higher PDI would be indicative of the occurrence of processes of aggregation/agglomeration and subsequent precipitation of the nanoparticles [37].

The initial zeta potential values obtained for the ALG/CS and CS/TPP nanoparticles were -28.2 ± 0.4 mV and $+27.0 \pm 3.0$ mV, respectively, with the values changing to -22.7 ± 0.9 mV and $+5.7 \pm 0.8$ mV, respectively, after 60 days (Fig. 3c). The initial value for the ALG/CS-GA$_3$ nanoparticles was -27.8 ± 0.9 mV, with a value of -27.1 ± 0.5 mV obtained after 60 days. In the case of the CS/TPP-GA$_3$ nanoparticles, the values were 25 ± 1.0 mV (initial) and 18.6 ± 0.5 mV (after 60 days). The zeta potential is one of the most important factors for the stability of nanoparticles; the higher the value, the greater the repulsion among the nanoparticles, which avoids aggregation/agglomeration [41].

The zeta potential depends on various factors; in the present case, as the pH of the nanoparticles did not change (Fig. 3d), the change in the zeta potential could have been due to rearrangements among the formulation components, notably the polymer chains. Meanwhile, an important point to stress is that the decrease was smaller in the presence of GA$_3$, indicating that the presence of this molecule probably led to better stabilization of the charges and

the groups responsible for intermolecular interactions among the components of the nanoparticles.

3.1.1. Release kinetics assays

The release kinetics tests showed that the nanoparticles of ALG/CS (pH 4.9) and CS/TPP (pH 4.7) modified the GA_3 release profile (Fig. 4a). Both nanoparticle systems showed 30% release after 8 h, while 80% release of the free GA_3 hormone occurred from the donor compartment to the acceptor compartment in 10 h. This same degree of release was reached after 17 h in the case of the ALG/CS-GA_3 nanoparticles, which therefore extended the release by 7 h. The CS/TPP system showed 54% release after 10 h, with no significant subsequent changes (Fig. 4a). The different release times can be explained by the nature of the chemical interactions between the active agent and the polymers, the hydrophilicity of the nanoparticles, and closing of the polymeric network [42]. The pKa values of the mannuronic and guluronic acid residues in the ALG polymer are 3.38 and 3.65, respectively [43], while the values are 6.5 for CS [44] and 4 for GA_3. The final pH of the nanoparticles (4.9) indicated that the GA_3 was deprotonated, enabling electrostatic interactions between the active agent and the surfaces of the CS/TPP nanoparticles (which presented a positive zeta potential). Stronger interactions that could maintain the active agent trapped inside the nanoparticles include hydrogen bonds between the amino groups of the CS polymer and the carboxylic acid group of GA_3.

The ALG/CS-GA_3 nanoparticles showed greater release, due to weaker interactions such as ionic bonds between the calcium ions used to produce the ALG gel with GA_3. Such interactions have been described for the encapsulation of other active principles using this type of nanoparticle [38,39]. Another contributing factor could be the internal hydrophilicity of the nanoparticles, as described by Aouada et al. [42] for the formation of hydrogels with the herbicide paraquat, where an increase of hydroxyl groups resulted in higher water uptake, relaxation of the polymeric matrix, and greater release of the herbicide. There was a higher presence of these groups in the ALG/CS-GA_3 nanoparticles, compared to CS/TPP-GA_3, which could have led to greater release, although 20% of the active agent remained trapped in the nanoparticles, probably due to stronger interaction between the polymer and the hormone. HPLC analyses did not show alterations in retention time or additional peaks for GA_3 during the kinetics assay, indicating that GA_3 remained stable after the preparation of the nanoparticles.

The mechanism of release of the hormone was investigated by applying the Korsmeyer-Peppas mathematical model [45]. The fitting for the ALG/CS-GA_3 nanoparticles resulted in a release kinetic constant (k) of $0.038 \, min^{-1}$ and a release exponent (n) of 1.26 (Fig. 4b, Table 1). The CS/TPP nanoparticles showed values of $k = 0.084 \, min^{-1}$ and $n = 0.87$ (Fig. 4c, Table 1), indicating that the release of GA_3 from the CS/TPP-GA_3 nanoparticles was faster, in the initial phase, compared to the release from the ALG/CS-GA_3 system. This corroborated the release kinetics data, where similar initial release profiles were obtained for the CS/TPP-GA_3 system and the free hormone.

According to the mathematical model, $n < 0.45$ indicates that the system releases the active agent by diffusion, following Fick's law; $n > 0.89$ indicates release by relaxation of the polymeric wall or erosion of the particle; and $0.45 < n < 0.89$ indicates release by anomalous transport, with both of the aforementioned mechanisms occurring simultaneously [45]. The CS/TPP-GA_3 nanoparticles therefore exhibited release by anomalous transport, while release from the ALG/CS-GA_3 system was due to relaxation or degradation of the polymeric matrix. The results of the mathematical treatment were in agreement with the release kinetics, where the CS/TPP nanoparticles showed faster release of GA_3, although the fact that 54% remained retained in the polymer indicated that

there was strong chemical interaction of GA_3 with a component of the CS/TPP nanoparticles.

Using an ALG/CS nanoparticle system as a carrier for the herbicide paraquat, Silva et al. [23] found nearly 100% release within 8 h, with the system presenting anomalous transport ($n = 0.83$) and a release kinetics constant (k) of $0.012 \, min^{-1}$. For release of paraquat from CS/TPP nanoparticles, Grillo et al. [12] showed that the release occurred by anomalous transport ($n = 0.60$), with faster release kinetics ($k = 1.99 \, min^{-1}$) than for the release of the same herbicide from ALG/CS nanoparticles; these values were similar to those found in the present work for CS/TPP nanoparticles loaded with GA_3.

Microparticulate and nanoparticulate systems are able to provide extended release profiles, compared to the use of free active agents, and as a result can maintain biological action for longer, increasing the effectiveness of the agent [46]. Another aspect of these systems is their potentially greater activity, because encapsulation increases the physical and chemical stability of the agent, protecting it from external factors that could cause degradation, such as photolysis or sorption [47,48]. The active agent therefore becomes more bioavailable and effective towards target organisms, enabling the use of lower applied concentrations to achieve the same effect, consequently helping to reduce contamination of the environment [8]. This is important, since agricultural chemicals can contaminate food, soil, and hydric resources [49]. In the case of GA_3, the use of nanocarriers provides protection against degradation caused by environmental factors such as light and temperature [21].

3.1.2. Release kinetics at different pH and temperature

The delivery systems were evaluated in terms of the effects of increased temperature and pH on the characteristics of the nanoparticles, the kinetics, and the release mechanism. Table 1 presents the characteristics of the nanoparticles at the end of the release tests under the different conditions of pH and temperature, together with the values of the release constant (k) and coefficient (n) obtained using the Korsmeyer-Peppas mathematical model.

With the rise of temperature, the ALG/CS-GA_3 nanoparticles showed increases in size as well as PDI, while these parameters remained unchanged for the CS/TPP nanoparticles. No changes in zeta potential were observed for either type of nanoparticle (Table 1).

After 8 h, the ALG/CS-GA_3 and CS/TPP-GA_3 nanoparticles showed releases of $81.8 \pm 0.43\%$ and $72.0 \pm 6.0\%$, respectively, when the assays were carried out at 30 °C (Fig. 5a). The release values were higher than obtained at room temperature. The release constant (k) values increased, while there were no changes in the release mechanisms, maintaining values of $n > 0.85$.

It has been found previously that a higher temperature alters the viscosity and hydrophilicity of polymers such as ALG and CS, which can be used to improve control of the release of an active agent [26,50]. This was not observed here for the carrier systems containing GA_3. It was reported by Liu et al. [51] that the release of GA_3 from the CS polymer was higher when the temperature was increased, due to loss of interaction between GA_3 and the amine group of CS.

At ambient temperature, the ALG/CS-GA_3 nanoparticles showed a reduced size at pH 5.9. At pH around 5.3, greater electrostatic interaction of the polymers produces nanoparticles that are more compact [52]. The PDI values were not affected, while the zeta potential shifted from $-31.6 \pm 1.31 \, mV$ to $-24.6 \pm 1.81 \, mV$. The increase of pH caused deprotonation of the carboxylic acid groups, consequently increasing the interaction with calcium ions present in these particles, making the zeta potential more positive [51].

For the CS/TPP-GA_3 nanoparticles, the pH change resulted in increased size and PDI. The closer the pH of the solution to the pKa
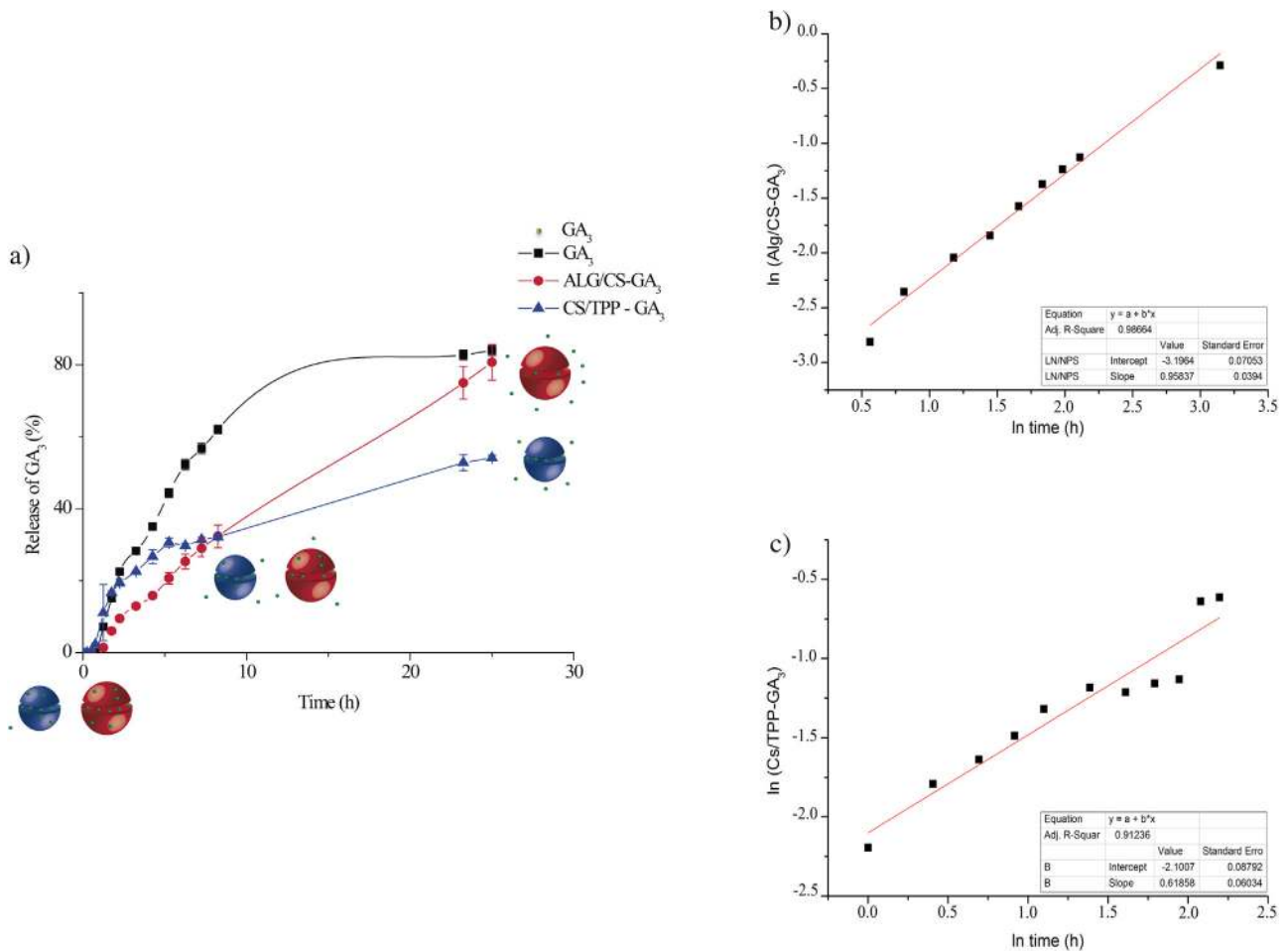
Fig. 4. a) Release profiles of free GA$_3$ and GA$_3$ encapsulated in the ALG/CS and CS/TPP nanoparticles (n = 3, 25 °C); b) fitting using the Korsmeyer–Peppas mathematical model applied to the release of GA$_3$ from the ALG/CS nanoparticles; c) fitting using the Korsmeyer–Peppas mathematical model applied to the release of GA$_3$ from the CS/TPP nanoparticles.

Table 1

Nanoparticles characterization at different pH and temperature, considering particle size, PDI, zeta potential, and the values obtained from the Korsmeyer-Peppas mathematical model for the kinetic constant (k) and release exponent (n).

	pH	Temperature (°C)	Size (nm)	PDI	Zeta potential (mV)	k (min^{-1})	n
ALG/CS-GA$_3$	4.9	25	471.8 ± 3.8	0.26 ± 0.01	−31.6 ± 1.31	0.038	1.26
	4.9	30	545.3 ± 23.6	0.36 ± 0.08	−35.2 ± 10.0	0.3894	3.56
	5.9	25	392.2 ± 7.7	0.28 ± 0.03	−27.3 ± 0.32	0.239	0.31
CS/TPP-GA$_3$	4.7	25	194 ± 4.2	0.31 ± 0.02	17.8 ± 0.94	0.084	0.87
	4.7	30	188.1 ± 2.78	0.23 ± 0.002	16.0 ± 1.05	0.264	4.0
	5.7	25	429.6 ± 1.63	0.44 ± 0.01	19.8 ± 0.41	0.254	0.28

of the CS polymer, the greater the tendency for precipitation of the polymer, leading to increased particle size or aggregation [53].

For both types of nanoparticles, the increase of pH accelerated the release of GA$_3$. After 8 h, the ALG/CS-GA$_3$ nanoparticles showed 57.4% release, while at pH 5.7, 78% release was obtained for the CS/TPP-GA$_3$ nanoparticles, which was close to the value obtained for free GA$_3$.

Release systems based on polyelectrolytic polymers are sensitive to pH changes, which can increase the release [54,55]. According to Mukhopadhyay et al. [55], alkaline media provide greater interaction of the solvent with the positive charge of CS, increasing penetration of the solvent into the nanoparticles and resulting in the release being governed by diffusion.

For both types of nanoparticles, the release constant values (k) increased with increasing pH, while the release exponent values for ALG/CS-GA$_3$ and CS/TPP-GA$_3$ decreased ($n < 0.45$), reflecting a shift

in the release mechanism from relaxation of the polymer matrix (or polymer degradation) to diffusion. The increase in pH led to increased release of GA$_3$ and a change in the release mechanism.

Both carrier systems were sensitive to changes in temperature and pH. These features are of interest for agricultural applications. As an example, the use of these formulations for seed treatment can enable modulation of the release of GA$_3$ from the nanoparticles in the field, due to the effects of factors such as temperature and pH.

3.2. Differential scanning calorimetry (DSC)

It can be seen that ALG, CS, TPP, and GA$_3$ presented phase transition/fusion peaks at 109, 101, 177, and 239 °C, respectively (Fig. 6). The endothermic peaks for the polymers were due to the loss of hydrophilic groups following decomposition of the polymers [22,56]. The ALG/CS nanoparticles, with and without GA$_3$, showed
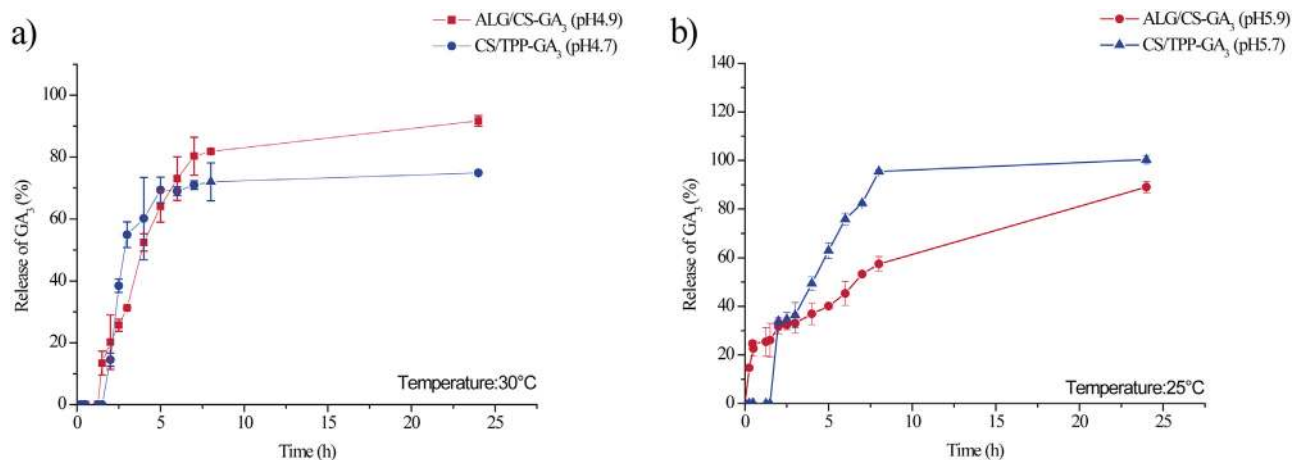
Fig. 5. Release profiles of GA$_3$ encapsulated in a) the ALG/CS (pH 4.9) and CS/TPP (pH 4.7) at temperature of 30 °C, and b) ALG/CS (pH 4.9) and CS/TPP nanoparticles (pH 5.7) at temperature of 25 °C.
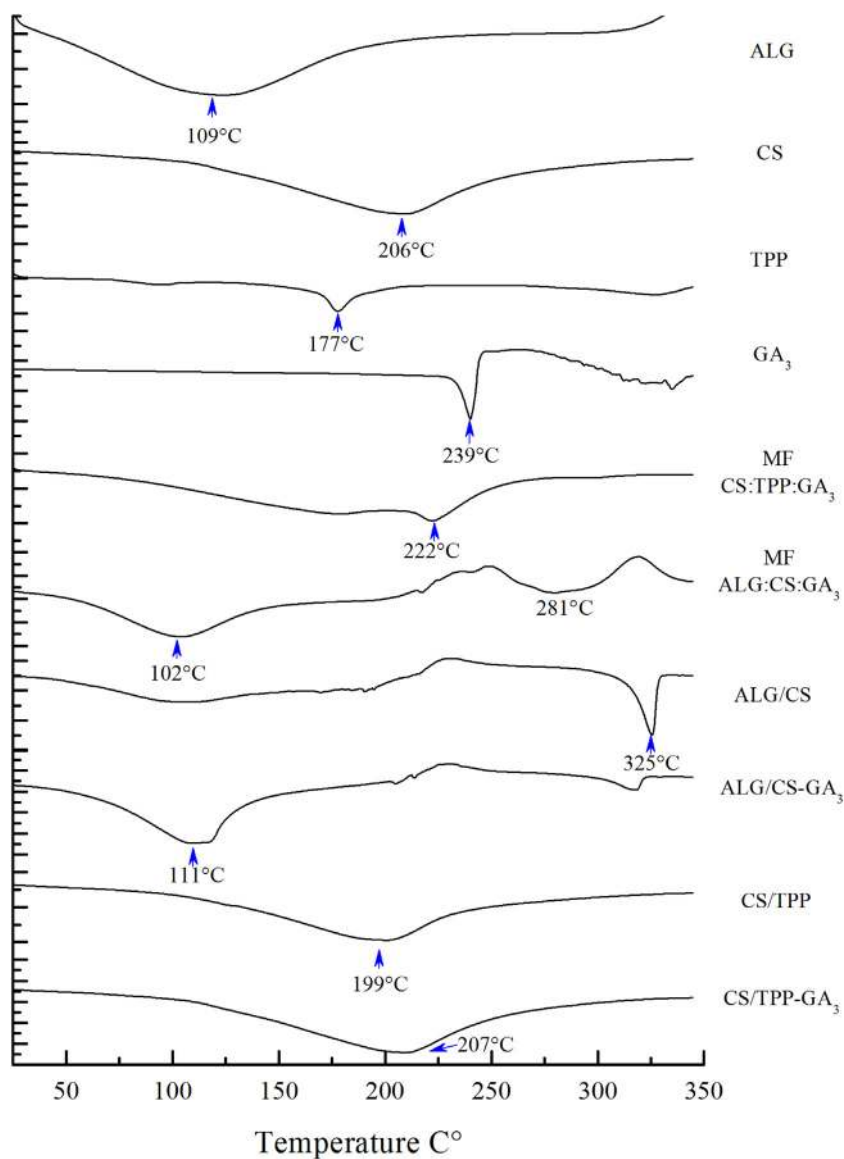

Fig. 6. Thermograms obtained by differential scanning calorimetry (DSC) for ALG, CS, TPP, GA$_3$, the physical mixture (MF), and ALG/CS and CS/TPP nanoparticles with and without GA$_3$. The samples were analyzed under a flow of nitrogen (50 mL min^{-1}), with heating at 10 °C min^{-1} in the temperature range 20–350 °C.
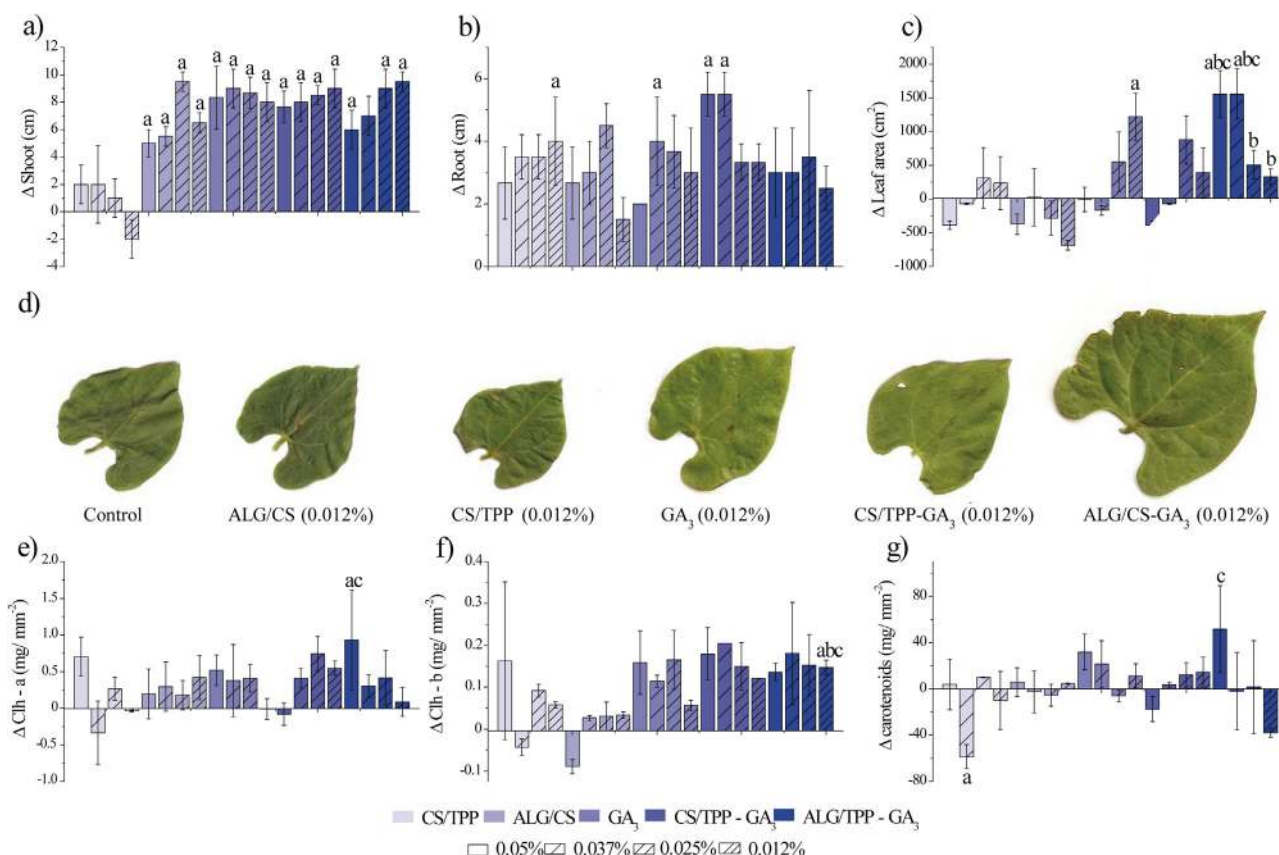
Fig. 7. Biological activities of the ALG/CS-GA$_3$ and CS/TPP-GA$_3$ nanoparticles towards *Phaseolus vulgaris*: a) shoot development (cm); b) root development (cm); c) leaf area development (cm^2); d) images of the leaves for the treatment at a concentration of 0.012%; e) chlorophyll 'a' content (mg mm^{-2}); f) chlorophyll 'b' content (mg mm^{-2}); g) total content of carotenoids (mg mm^{-2}). Statistical analysis using one-way ANOVA with Tukey's post-hoc test (p < 0.05), where **a** indicates significant difference relative to the control, **b** indicates significant difference relative to the nanoparticles without GA$_3$, and **c** indicates significant difference relative to free GA$_3$.

an endothermic peak at 325 °C, which was higher than reported previously for ALG/CS nanoparticles. Fattahpour et al. [57] found that ALG/CS nanoparticles presented a new endothermic peak at 302.8 °C, with no appearance of the endothermic peaks of the ALG and CS polymers. Silva et al. [23] found that ALG/CS nanoparticles used as carriers for paraquat presented an endothermic peak at 70 °C, which was slightly higher compared to the physical mixture of the pure polymers, which showed peaks for ALG at 62 °C and CS at 68 °C. Emami et al. [58] reported an endothermic peak for ALG/CS nanoparticles at 210.45 °C, different to the peaks associated with the polymers, which was attributed to polyelectrolytic complexation between the polymers. These findings revealed that strong interaction in the ALG/CS nanoparticles prepared in this study acted to raise the fusion point, compared to the values for the individual polymers.

The CS/TPP nanoparticles showed broad endothermic peaks at around 199 and 207 °C in the absence and presence of GA$_3$, respectively, which were close to the value for the CS polymer (206 °C). The lower temperature for the CS/TPP nanoparticles without GA$_3$ was consistent with earlier findings [59], where the lower temperature endothermic peak of CS/TPP (compared to the polymer) was attributed to the loss of crystallinity of CS, which was converted to its amorphous form. Loading with GA$_3$ caused no change in the values, compared to the pure polymer, suggesting that the GA$_3$ was dispersed in the polymeric matrix of the nanoparticles.

3.3. Biological activity

The results (Fig. 7) showed that the treatments with free GA$_3$ or the nanoparticles loaded with GA$_3$ promoted shoot development in all cases (without any statistical differences among them), with an average 8.2 cm increase in length, compared to the control (Fig. 7a). The findings indicated that the carrier system possessed biological activity similar to that of the free hormone. A notable feature was that the effect obtained using the ALG/CS nanoparticles alone, without any hormone, was similar to the effect in the presence of the hormone (this was not observed in the case of the CS/TPP nanoparticles). The composition of the ALG/CS nanoparticles included CaCl$_2$, which has previously been studied for the alleviation of plant stress in dry [60] or saline [61] environments. According to Wang et al. [62], exogenous application of CaCl$_2$ to soybean plants at a concentration of 6 mM resulted in increased quality and size of the plant, as well as increased endogenous levels of the hormones gibberellic acid and indole-acetic acid. In the case of the ALG/CS nanoparticles, the CaCl$_2$ concentration of 50 mM could have caused initial plant growth similar to that obtained in the treatments with GA$_3$. Qureshi et al. [63] found that the use of exogenous GA$_3$ increased the number of leaves and the leaf area, and in combination with CaCl$_2$ resulted in greater plant mass. The fact that the ALG/CS nanoparticles contained CaCl$_2$ in their structure could have led to similar effects.

In the case of root development, only the free hormone (at a concentration of 0.025%) and the CS/TPP-GA$_3$ nanoparticles (at concentrations of 0.012 and 0.025%) caused different growth rates, relative to the control, with increases in root length of 4, 5.5, and 5.5 cm, respectively (Fig. 7b). The development of the roots is critical for the plant, since they are responsible for the uptake of nutrients and water from the soil [64], and in agricultural crops a more extensive root network enables faster absorption of fertilizers, improving plant quality [65].

In the case of leaf area (Fig. 7c), the free hormone at a concentration of 0.05% increased growth, relative to the control, while use of the ALG/CS-GA$_3$ nanoparticles at concentrations of 0.012 and 0.025% led to greater leaf area, compared to use of the free hormone or the CS/TPP-GA$_3$ nanoparticles (Fig. 7d). At these two dilutions, use of the ALG/CS-GA$_3$ carrier system led to an average leaf area that was 78% higher than the control, and the effectiveness of ALG/CS-GA$_3$ was 82% higher than that of the free hormone. A larger leaf area results in increased capture of sunlight and increases photosynthesis, so more energy is available for plant growth [66]. In the present case using *Phaseolus vulgaris*, the CS/TPP-GA$_3$ system exerted an effect on root development, while the ALG/CS-GA$_3$ nanoparticles acted to increase leaf area.

The nanoparticle systems presented different effects on the pigment contents. An important finding was that the ALG/CS-GA$_3$ nanoparticles at a concentration of 0.012% acted to increase the levels of chlorophyll 'a', relative to the control, while the CS/TPP-GA$_3$ nanoparticles at a concentration of 0.05% increased the levels of chlorophyll 'b', relative to the control, the free hormone, and the CS/TPP-GA$_3$ nanoparticles (Fig. 7e and f). At a concentration of 0.012%, the ALG/CS-GA$_3$ nanoparticles acted to increase the content of carotenoids, while the other treatments showed no differences, relative to the control (Fig. 7g). The effects observed for *Phaseolus vulgaris*, using GA$_3$ at levels equivalent to those applied in agriculture, revealed the alteration of biochemical processes in the plants, with accelerated plant development and increased levels of chlorophylls and carotenoids [67,68]. For all the parameters evaluated, the ALG/CS nanocarrier system showed better performance, compared to the free hormone or the CS/TPP system, with the lowest concentration (0.012%) being most suitable.

The carrier systems used in this study presented different physical characteristics (size and zeta potential) and release mechanisms, resulting in different morphological and biochemical effects in *Phaseolus vulgaris*, although both systems have potential for use in agriculture. The different release mechanisms had an important influence on their effects, with the faster release from the ALG/CS-GA$_3$ nanoparticles system probably resulting in a greater short-term effect. In the CS/TPP-GA$_3$ system, stronger interactions caused extended retention of the hormone, with slower release, which could lead to greater effects after periods longer than used in this study.

Only a few nanocarrier systems for use with plant growth regulators have been described in the literature, and most studies have only concerned system characterization. In contrast to previous investigations, the present work evaluates the physical-chemical characteristics of two different carrier systems and also identifies the system that provided the best biological efficacy.

Nanocarrier systems provide more efficient delivery of active agents in agricultural field applications, compared to conventional products [14,69]. There have been few studies of carriers for plant hormones [19,70,71], but these systems have broad potential for use in the field, offering improved chemical stability and bioavailability. In the present case, the nanoparticle systems evaluated were shown to be able to provide effective delivery of the GA$_3$ plant hormone to crops.

4. Conclusions

This work describes nanoparticle systems composed of ALG/CS or CS/TPP as carriers for the GA$_3$ plant hormone. Both systems provided highly efficient encapsulation of GA$_3$. The hormone release profiles were different for the two systems, with the initial release being slower from the ALG/CS nanoparticles than from the CS/TPP nanoparticles, because the latter interacted more strongly with GA$_3$. The release of GA$_3$ was altered following changes of temperature and pH. DSC analyses confirmed interaction of the hormone with the carrier systems. In biological activity assays using *Phaseolus vulgaris*, the ALG/CS-GA$_3$ nanoparticles showed stronger effects, in terms of leaf development and the level of carotenoids, compared to the free hormone or the CS/TPP-GA$_3$ nanoparticles. The ALG/CS and CS/TPP nanoparticles showed different physical characteristics (size and zeta potential), resulting in different biological effects. Further studies of these two systems should be undertaken at different stages of development of *Phaseolus vulgaris* and other plant species, and toxicity assays should be performed. Given the wide range of functions of GA$_3$ during the different stages of plant development, future studies may indicate diverse applications of CS/TPP-GA$_3$ and ALG/CS-GA$_3$ NPs in agriculture, such as in increased plant fertility [72], the formation of parthenocarpic fruits [73], and promotion of the germination of seeds that present physiological dormancy [74]. In particular, the use of nanoparticulate systems for this hormone could ensure greater biological activity and efficiency in the field, resulting in higher quality, increased production, and greater economic value of agricultural products.

References

[1] W. Rademacher, Plant growth regulators: backgrounds and uses in plant production, J. Plant Growth Regul. 34 (2015) 845–872, http://dx.doi.org/10.1007/s00344-015-9541-6.

[2] E. Nambara, Plant hormones, in: S.M. Hughes (Ed.), Brenner's Encyclopedia of Genetics, Second ed., Academic Press, San Diego, 2013, pp. 346–348, http://www.sciencedirect.com/science/article/pii/B9780123749840011700 (Accessed 28 October 2014).

[3] P. Hedden, V. Sponsel, A century of gibberellin research, J. Plant Growth Regul. 34 (2015) 740–760, http://dx.doi.org/10.1007/s00344-015-9546-1.

[4] P. Hedden, V. Sponsel, A century of gibberellin research, J. Plant Growth Regul. 34 (2015) 740–760, http://dx.doi.org/10.1007/s00344-015-9546-1.

[5] C. Reig, V. Farina, G. Volpe, C. Mesejo, A. Martínez-Fuentes, F. Barone, F. Calabrese, M. Agustí, Gibberellic acid and flower bud development in loquat (Eriobotrya japonica Lindl.), Sci. Hortic. 129 (2011) 27–31, http://dx.doi.org/10.1016/j.scienta.2011.02.017.

[6] P. Teszlák, M. Kocsis, K. Gaál, M.P. Nikfardjam, Regulatory effects of exogenous gibberellic acid (GA3) on water relations and CO2 assimilation among grapevine (Vitis vinifera L.) cultivars, Sci. Hortic. 159 (2013) 41–51, http://dx.doi.org/10.1016/j.scienta.2013.04.037.

[7] M. Kah, T. Hofmann, Nanopesticide research: current trends and future priorities, Environ. Int. 63 (2014) 224–235, http://dx.doi.org/10.1016/j.envint.2013.11.015.

[8] L.R. Khot, S. Sankaran, J.M. Maja, R. Ehsani, E.W. Schuster, Applications of nanomaterials in agricultural production and crop protection: a review, Crop Prot. 35 (2012) 64–70, http://dx.doi.org/10.1016/j.cropro.2012.01.007.

[9] M. Rossi, F. Cubadda, L. Dini, M.L. Terranova, F. Aureli, A. Sorbo, D. Passeri, Scientific basis of nanotechnology, implications for the food sector and future trends, Trends Food Sci Technol. 40 (2014) 127–148, http://dx.doi.org/10.1016/j.tifs.2014.09.004.

[10] R. Grillo, P.C. Abhilash, L.F. Fraceto, Nanotechnology applied to bio-encapsulation of pesticides, J. Nanosci. Nanotechnol. 16 (2016) 1231–1234, http://dx.doi.org/10.1166/jnn.2016.12332.

[11] E.V.R. Campos, J.L. de Oliveira, L.F. Fraceto, Applications of controlled release systems for fungicides, herbicides, acaricides, nutrients, and plant growth hormones: a review, Adv. Sci. Eng. Med. 6 (2014) 373–387, http://dx.doi.org/10.1166/asem.2014.1538.

[12] R. Grillo, A.E.S. Pereira, C.S. Nishisaka, R. de Lima, K. Oehlke, R. Greiner, L.F. Fraceto, Chitosan/tripolyphosphate nanoparticles loaded with paraquat herbicide: an environmentally safer alternative for weed control, J. Hazard. Mater. 278 (2014) 163–171, http://dx.doi.org/10.1016/j.jhazmat.2014.05.079.

[13] E.V.R. Campos, J.L. de Oliveira, C.M.G. da Silva, M. Pascoli, T. Pasquoto, R. Lima, P.C. Abhilash, L. Fernandes Fraceto, Polymeric and solid lipid nanoparticles for sustained release of carbendazim and tebuconazole in agricultural applications, Sci. Rep. 5 (2015), http://dx.doi.org/10.1038/srep13809.

[14] C.R. Maruyama, M. Guilger, M. Pascoli, N. Bileshy-José, P.C. Abhilash, L.F. Fraceto, R. de Lima, Nanoparticles based on chitosan as carriers for the

combined herbicides imazapic and imazapyr, Sci. Rep. 6 (2016) 19768, http://dx.doi.org/10.1038/srep19768.

[15] P.L. Kashyap, X. Xiang, P. Heiden, Chitosan nanoparticle based delivery systems for sustainable agriculture, Int. J. Biol. Macromol. 77 (2015) 36–51, http://dx.doi.org/10.1016/j.ijbiomac.2015.02.039.

[16] L.Y. Ing, N.M. Zin, A. Sarwar, H. Katas, Antifungal activity of chitosan nanoparticles and correlation with their physical properties, Int. J. Biomater. (2012) e632698, http://dx.doi.org/10.1155/2012/632698.

[17] M. Sathiyabama, R. Parthasarathy, Biological preparation of chitosan nanoparticles and its in vitro antifungal efficacy against some phytopathogenic fungi, Carbohydr. Polym. 151 (2016) 321–325, http://dx.doi.org/10.1016/j.carbpol.2016.05.033.

[18] Y.-I. Jeong, S.-J. Seo, I.-K. Park, H.-C. Lee, I.-C. Kang, T. Akaike, C.-S. Cho, Cellular recognition of paclitaxel-loaded polymeric nanoparticles composed of poly(γ-benzyl l-glutamate) and poly(ethylene glycol) diblock copolymer endcapped with galactose moiety, Int. J. Pharm. 296 (2005) 151–161, http://dx.doi.org/10.1016/j.ijpharm.2005.02.027.

[19] J.P. Quiñones, Y.C. García, H. Curiel, C.P. Covas, Microspheres of chitosan for controlled delivery of brassinosteroids with biological activity as agrochemicals, Carbohydr. Polym. 80 (2010) 915–921, http://dx.doi.org/10.1016/j.carbpol.2010.01.006.

[20] S. Tao, R. Pang, C. Chen, X. Ren, S. Hu, Synthesis, characterization and slow release properties of O-naphthylacetyl chitosan, Carbohydr. Polym. 88 (2012) 1189–1194, http://dx.doi.org/10.1016/j.carbpol.2012.01.076.

[21] Y. Liu, Y. Sun, S. He, Y. Zhu, M. Ao, J. Li, Y. Cao, Synthesis and characterization of gibberellin–chitosan conjugate for controlled-release applications, Int. J. Biol. Macromol. 57 (2013) 213–217, http://dx.doi.org/10.1016/j.ijbiomac.2013.03.024.

[22] B. Sarmento, D. Ferreira, F. Veiga, A. Ribeiro, Characterization of insulin-loaded alginate nanoparticles produced by ionotropic pre-gelation through DSC and FTIR studies, Carbohydr. Polym. 66 (2006) 1–7, http://dx.doi.org/10.1016/j.carbpol.2006.02.008.

[23] M. dos, S. Silva, D.S. Cocenza, N.F.S. de Melo, R. Grillo, A.H. Rosa, L.F. Fraceto, Alginate nanoparticles as a controlled release system for clomazone herbicide, Quim. Nova 33 (2010) 1868–1873.

[24] S. Tripathy, S. Das, S.P. Chakraborty, S.K. Sahu, P. Pramanik, S. Roy, Synthesis, characterization of chitosan–tripolyphosphate conjugated chloroquine nanoparticle and its in vivo anti-malarial efficacy against rodent parasite: a dose and duration dependent approach, Int. J. Pharm. 434 (2012) 292–305, http://dx.doi.org/10.1016/j.ijpharm.2012.05.064.

[25] T. Jiang, R. James, S.G. Kumbar, C.T. Laurencin, Chapter 5 – chitosan as a biomaterial: structure, properties, and applications in tissue engineering and drug delivery, in: S.G.K.T.L. Deng (Ed.), Nat. Synth. Biomed. Polym., Elsevier, Oxford, 2014, pp. 91–113, http://www.sciencedirect.com/science/article/pii/B9780123969835000053 (Accessed 3 December 2014).

[26] M.A. Azevedo, A.I. Bourbon, A.A. Vicente, M.A. Cerqueira, Alginate/chitosan nanoparticles for encapsulation and controlled release of vitamin B2, Int. J. Biol. Macromol. 71 (2014) 141–146, http://dx.doi.org/10.1016/j.ijbiomac.2014.05.036.

[27] P. Calvo, C. Remuñán-López, J.L. Vila-Jato, M.J. Alonso, Novel hydrophilic chitosan-polyethylene oxide nanoparticles as protein carriers, J. Appl. Polym. Sci. 63 (1997) 125–132, http://dx.doi.org/10.1002/(SICI)1097-4628(19970103)63:1<125:AID-APP13>3.0.CO;2-4.

[28] J. Siepmann, N.A. Peppas, Modeling of drug release from delivery systems based on hydroxypropyl methylcellulose (HPMC), Adv. Drug Deliv. Rev. 48 (2001) 139–157, http://dx.doi.org/10.1016/S0169-409X(01)00112-0.

[29] C. Rodrigues, L.P. de S. Vandenberghe, J. de Oliveira, C.R. Soccol, New perspectives of gibberellic acid production: a review, Crit. Rev. Biotechnol. 32 (2012) 263–273, http://dx.doi.org/10.3109/07388551.2011.615297.

[30] A.D. Pavlista, D.K. Santra, J.A. Schild, G.W. Hergert, Gibberellic acid sensitivity among common bean cultivars (Phaseolus vulgaris L.), HortScience 47 (2012) 637–642.

[31] A.R. Wellburn, The spectral determination of chlorophylls a and b, as well as total carotenoids, using various solvents with spectrophotometers of different resolution, J. Plant Physiol. 144 (1994) 307–313, http://dx.doi.org/10.1016/S0176-1617(11)81192-2.

[32] J.A. Gallego-Urrea, J. Tuoriniemi, M. Hassellöv, Applications of particle-tracking analysis to the determination of size distributions and concentrations of nanoparticles in environmental, biological and food samples, TrAC Trends Anal. Chem. 30 (2011) 473–483, http://dx.doi.org/10.1016/j.trac.2011.01.005.

[33] V. Filipe, A. Hawe, W. Jiskoot, Critical evaluation of Nanoparticle Tracking Analysis (NTA) by NanoSight for the measurement of nanoparticles and protein aggregates, Pharm. Res. 27 (2010) 796–810, http://dx.doi.org/10.1007/s11095-010-0073-2.

[34] S. Vimal, S. Abdul Majeed, G. Taju, K.S.N. Nambi, N. Sundar Raj, N. Madan, M.A. Farook, T. Rajkumar, D. Gopinath, A.S. Sahul Hameed, Chitosan tripolyphosphate (CS/TPP) nanoparticles: preparation, characterization and application for gene delivery in shrimp, Acta Trop. 128 (2013) 486–493, http://dx.doi.org/10.1016/j.actatropica.2013.07.013.

[35] A. Rampino, M. Borgogna, P. Blasi, B. Bellich, A. Cesàro, Chitosan nanoparticles: preparation, size evolution and stability, Int. J. Pharm. 455 (2013) 219–228, http://dx.doi.org/10.1016/j.ijpharm.2013.07.034.

[36] J.R. Costa, N.C. Silva, B. Sarmento, M. Pintado, Potential chitosan-coated alginate nanoparticles for ocular delivery of daptomycin, Eur. J. Clin. Microbiol. Infect. Dis. 34 (2015) 1255–1262, http://dx.doi.org/10.1007/s10096-015-2344-7.

[37] L. Wu, J. Zhang, W. Watanabe, Physical and chemical stability of drug nanoparticles, Adv. Drug Deliv. Rev. 63 (2011) 456–469, http://dx.doi.org/10.1016/j.addr.2011.02.001.

[38] N.F.S. de Melo, E.V.R. Campos, E. de Paula, A.H. Rosa, L.F. Fraceto, Factorial design and characterization studies for articaine hydrochloride loaded alginate/chitosan nanoparticles, J. Colloids Sci. Biotechnol. 2 (2013) 146–152, http://dx.doi.org/10.1166/jcsb.2013.1048.

[39] C.B. Woitiski, F. Veiga, A. Ribeiro, R. Neufeld, Design for optimization of nanoparticles integrating biomaterials for orally dosed insulin, Eur. J. Pharm. Biopharm. Off. J. Arbeitsgemeinschaft Für Pharm. Verfahrenstechnik E.V. 73 (2009) 25–33, http://dx.doi.org/10.1016/j.ejpb.2009.06.002.

[40] V. Arulmozhi, K. Pandian, S. Mirunalini, Ellagic acid encapsulated chitosan nanoparticles for drug delivery system in human oral cancer cell line (KB), Colloids Surf. B Biointerfaces 110 (2013) 313–320, http://dx.doi.org/10.1016/j.colsurfb.2013.03.039.

[41] S. Honary, F. Zahir, Effect of zeta potential on the properties of nano-drug delivery systems – a review (Part 2), Trop. J. Pharm. Res. 12 (2013), http://dx.doi.org/10.4314/tjpr.v12i2.20.

[42] F.A. Aouada, M.R. de Moura, W.J. Orts, L.H.C. Mattoso, Polyacrylamide and methylcellulose hydrogel as delivery vehicle for the controlled release of paraquat pesticide, J. Mater. Sci. 45 (2010) 4977–4985, http://dx.doi.org/10.1007/s10853-009-4180-6.

[43] J.P. Fuenzalida, P.K. Nareddy, I. Moreno-Villoslada, B.M. Moerschbacher, M.J. Swamy, S. Pan, M. Ostermeier, F.M. Goycoolea, On the role of alginate structure in complexing with lysozyme and application for enzyme delivery, Food Hydrocolloids 53 (2016) 239–248, http://dx.doi.org/10.1016/j.foodhyd.2015.04.017.

[44] H.-W. Sung, K. Sonaje, Z.-X. Liao, L.-W. Hsu, E.-Y. Chuang, pH-responsive nanoparticles shelled with chitosan for oral delivery of insulin: from mechanism to therapeutic applications, Acc. Chem. Res. 45 (2012) 619–629, http://dx.doi.org/10.1021/ar200234q.

[45] R.W. Korsmeyer, R. Gurny, E. Doelker, P. Buri, N.A. Peppas, Mechanisms of solute release from porous hydrophilic polymers, Int. J. Pharm. 15 (1983) 25–35, http://dx.doi.org/10.1016/0378-5173(83)90064-9.

[46] M. Fernández-Pérez, F.J. Garrido-Herrera, E. González-Pradas, Alginate and lignin-based formulations to control pesticides leaching in a calcareous soil, J. Hazard. Mater. 190 (2011) 794–801, http://dx.doi.org/10.1016/j.jhazmat.2011.03.118.

[47] M. Cea, P. Cartes, G. Palma, M.L. Mora, Atrazine efficiency in an andisol as affected by clays and nanoclays in ethylcellulose controlled release formulations, Rev. Cienc. Suelo Nutr. Veg. 10 (2010) 62–77.

[48] H.M. Nguyen, I.C. Hwang, J.W. Park, H.J. Park, Enhanced payload and photo-protection for pesticides using nanostructured lipid carriers with corn oil as liquid lipid, J. Microencapsul. 29 (2012) 596–604, http://dx.doi.org/10.3109/02652048.2012.668960.

[49] J. Schmitz, M. Hahn, C.A. Brühl, Agrochemicals in field margins – an experimental field study to assess the impacts of pesticides and fertilizers on a natural plant community, Agric. Ecosyst. Environ. 193 (2014) 60–69, http://dx.doi.org/10.1016/j.agee.2014.04.025.

[50] P.B. Kajjari, L.S. Manjeshwar, T.M. Aminabhavi, Novel pH- and temperature-responsive blend hydrogel microspheres of sodium alginate and PNIPAAm-g-GG for controlled release of isoniazid, AAPS PharmSciTech 13 (2012) 1147–1157, http://dx.doi.org/10.1208/s12249-012-9838-8.

[51] Y. Y. Liu, Y. Sun, H. Xu, S. Feng, J. Fu, W. Tang, D. Liu, H. Sun, S. Xu Jiang, Preparation and evaluation of lysozyme-loaded nanoparticles coated with poly-γ-glutamic acid and chitosan, Int. J. Biol. Macromol. 59 (2013) 201–207, http://dx.doi.org/10.1016/j.ijbiomac.2013.04.065.

[52] T. Gazori, M.R. Khoshayand, E. Azizi, P. Yazdizade, A. Nomani, I. Haririan, Evaluation of alginate/chitosan nanoparticles as antisense delivery vector: formulation, optimization and in vitro characterization, Carbohydr. Polym. 77 (2009) 599–606, http://dx.doi.org/10.1016/j.carbpol.2009.02.019.

[53] D.A. Körpe, S. Malekghasemi, U. Aydın, M. Duman, Fabrication of monodispersive nanoscale alginate–chitosan core–shell particulate systems for controlled release studies, J. Nanopart. Res. 16 (2014), http://dx.doi.org/10.1007/s11051-014-2754-y.

[54] D. Natrajan, S. Srinivasan, K. Sundar, A. Ravindran, Formulation of essential oil-loaded chitosan–alginate nanocapsules, J. Food Drug Anal. 23 (2015) 560–568, http://dx.doi.org/10.1016/j.jfda.2015.01.001.

[55] P. Mukhopadhyay, S. Chakraborty, S. Bhattacharya, R. Mishra, P.P. Kundu, pH-sensitive chitosan/alginate core-shell nanoparticles for efficient and safe oral insulin delivery, Int. J. Biol. Macromol. 72 (2015) 640–648, http://dx.doi.org/10.1016/j.ijbiomac.2014.08.040.

[56] A.P. Bagre, K. Jain, N.K. Jain, Alginate coated chitosan core shell nanoparticles for oral delivery of enoxaparin: in vitro and in vivo assessment, Int. J. Pharm. 456 (2013) 31–40, http://dx.doi.org/10.1016/j.ijpharm.2013.08.037.

[57] S. Fattahpour, M. Shamanian, N. Tavakoli, M. Fathi, S.R. Sheykhi, S. Fattahpour, Design and optimization of alginate-chitosan-pluronic nanoparticles as a novel meloxicam drug delivery system, J. Appl. Polym. Sci. 132 (2015), http://dx.doi.org/10.1002/app.42241, n/a–n/a.

[58] J. Emami, M.S.S. Boushehri, J. Varshosaz, Preparation, characterization and optimization of glipizide controlled release nanoparticles, Res. Pharm. Sci. 9 (2014) 301–314.

[59] S. Fazil, S. Md, M. Haque, S. Baboota, J. kaur Sahni, Development and evaluation of rivastigmine loaded chitosan nanoparticles for brain targeting,

Eur. J. Pharm Sci. 47 (2012) 6–15, http://dx.doi.org/10.1016/j.ejps.2012.04.013.

[60] X.-Y. Cai, X.-D. Chen, C.-Z. Li, C. Liu, Effects of exogenous Ca2+ on the seed germination of Koelreuteria paniculata in limestone area of Southwest China under drought stress, J. Appl. Ecol. 24 (2013) 1341–1346.

[61] D.-H. Han, S.-J. Li, E.-J. Wang, H.-M. Meng, Y. Chen, Y. Zhang, Effect of exogenous calcium on seed germination and seedling physiological characteristics of Lycium ruthenium, Zhongguo Zhong Yao Za Zhi Zhongguo Zhongyao Zazhi China J. Chin. Mater. Med. 39 (2014) 34–39.

[62] X. Wang, R. Yang, X. Jin, C. Shen, Y. Zhou, Z. Chen, Z. Gu, Effect of supplemental Ca2+ on yield and quality characteristics of soybean sprouts, Sci. Hortic. 198 (2016) 352–362, http://dx.doi.org/10.1016/j.scienta.2015.11.022.

[63] K.M. Qureshi, S. Chughtai, U.S. Qureshi, N.A. Abbasi, Impact of exogenous application of salt and growth regulators on growth and yield of strawberry, Pak. J. Bot. 45 (2013) 1179–1185.

[64] L.V. Kochian, Root architecture, J. Integr. Plant Biol. 58 (3) (2016) 190–192, http://dx.doi.org/10.1111/jipb.12471.

[65] J.P. Lynch, K.M. Brown, New roots for agriculture: exploiting the root phenome, Philos. Trans. R. Soc. Lond. B Biol. Sci. 367 (2012) 1598–1604, http://dx.doi.org/10.1098/rstb.2011.0243.

[66] J.D. Lima, N.F. Ansante, E.S. Nomura, E.J. Fuzitani, S.H.M.-G. da Silva, J.D. Lima, N.F. Ansante, E.S. Nomura, E.J. Fuzitani, S.H.M.-G. da Silva, Growth and yield of anthurium in response to gibberellic acid, Ciênc Rural 44 (2014) 1327–1333, http://dx.doi.org/10.1590/0103-8478cr20120586.

[67] M.A. Awad, A.D. Al-Qurashi, Gibberellic acid spray and bunch bagging increase bunch weight and improve fruit quality of Barhee date palm cultivar under hot arid conditions, Sci. Hortic. 138 (2012) 96–100, http://dx.doi.org/10.1016/j.scienta.2012.02.015.

[68] Y.-X. Zang, I.-J. Chun, L.-L. Zhang, S.-B. Hong, W.-W. Zheng, K. Xu, Effect of gibberellic acid application on plant growth attributes, return bloom, and fruit quality of rabbiteye blueberry, Sci. Hortic. 200 (2016) 13–18, http://dx.doi.org/10.1016/j.scienta.2015.12.057.

[69] J.L. de Oliveira, E.V.R. Campos, C.M. Gonçalves da Silva, T. Pasquoto, R. Lima, L.F. Fraceto, Solid lipid nanoparticles Co-loaded with simazine and atrazine: preparation, characterization, and evaluation of herbicidal activity, J. Agric. Food Chem. 63 (2015) 422–432, http://dx.doi.org/10.1021/jf5059045.

[70] E.M. Smoak, A.D. Carlo, C.C. Fowles, I.A. Banerjee, Self-assembly of gibberellic amide assemblies and their applications in the growth and fabrication of ordered gold nanoparticles, Nanotechnology 21 (2010) 25603, http://dx.doi.org/10.1088/0957-4484/21/2/025603.

[71] S. Tao, R. Pang, C. Chen, X. Ren, S. Hu, Synthesis, characterization and slow release properties of O-naphthylacetyl chitosan, Carbohydr. Polym. 88 (2012) 1189–1194, http://dx.doi.org/10.1016/j.carbpol.2012.01.076.

[72] C.-T. Kwon, N.-C. Paek, Gibberellic acid: a key phytohormone for spikelet fertility in rice grain production, Int. J. Mol. Sci. 17 (2016), http://dx.doi.org/10.3390/ijms17050794.

[73] M.C.T. Pereira, J.H. Crane, S. Nietsche, W. Montas, M.A. Santos, Reguladores de crescimento na frutificação efetiva e qualidade de frutos partenocárpicos de atemoia Gefner, Pesqui, Agropecuária Bras. 49 (2014) 281–289, http://dx.doi.org/10.1590/S0100-204X2014000400006.

[74] K. Shu, X. Liu, Q. Xie, Z. He, Two faces of one seed: hormonal regulation of dormancy and germination, Mol. Plant. 9 (2016) 34–45, http://dx.doi.org/10.1016/j.molp.2015.08.010.